DOI: 10.19184/ICL.v2i1.367

Hydrothermal Synthesis of Hematite (α-Fe_2O_3) from Indonesia Iron Sand

Furqonul Hakin Al Hadi[a], Tanti Haryati[a], Novita Andarini[a], Suwardiyanto[a], Yudi Aris Sulistiyo*[a]

Abstract: High potency of Indonesian iron sand can be optimized by transforming to valuable iron oxide product namely Hematite (α-Fe_2O_3). Hydrothermal synthesis was carried out to transform iron oxide phase to hematite that can be analyzed by x-ray diffraction method. Utilization of ion sand as raw material produced multyphase in product reaction, while the usage of $Fe(OH)_x$ that extracted from iron sand attained high purity of hematite. The best conditions of reaction were at 160 °C for 24 h. Higher temperature and longer time reaction transformed α- α-Fe_2O_3 to be γ-Al_2O_3 and Fe_3O_4 as more stable phase.

Keywords: Iron sand, hematite, α-Fe_2O_3, hydrothermal synthesis.

INTRODUCTION

Indonesia's Iron sand abundancy is deposited in several areas such as Sumatra, South of Jawa, Sulawesi, Maluku, and Papua that possibly produced from volcanic eruption and erosion of older rock [1]. In 2020, Ministry of Energy and Mineral Resources of the Republic of Indonesia reported the amount of Iron sand resources in Indonesia is 2.9 Billion tons and supply 1.7% of world Iron sand that the iron content was less than 12% [2]. However, Zulhan et al. (2021) reported the mined and concentrated iron sand deposits in some areas contained more than 54% iron and 7% titanium [3]. Iron sand can be utilized in various applications namely steel manufacturing, pigment Sources [4], titanium feedstock [5], adsorbent for water purification [6-8].

In particularly, iron oxides have large potential applications in data storage, biotechnology, biomedicine, catalyst, sersors, and environmental remediation due to its unique physical and chemical properties [9]. Regarding the most oxidation state of iron (Fe^{2+} and Fe^{3+}), iron oxides have three common form that is Hematite (α-Fe_2O_3), maghemite (Fe_3O_4), and magnetite (γ-Fe_2O_3) [10]. Among these, the hematite is most environmentally friendly as a semiconductor materials (e.g., 2.1 eV) [11-12]. The stability of Hematite was determined from the rombohedral structure with the latyice oxygen close packing and two third of the lattice was occupy with the Fe^{3+} ions [13].

Among various synthesis methods of hematite, the hydrothermal method is one of the most common and the least expensive routes of synthesizing nanoparticles with different morphologies. Recently, hematite was synthezed by the bottom-up model using iron ion (Fe^{3+}) under supercritical condition [14-15]. To the best of our knowledge, few scientific paper reported the top-down model from the iron sand using hydrothermal syntesis teqnique. The challenge of top-down model is the iron sand has several iron oxide phase and also other oxide that possibly interfere the production of α-Fe_2O_3. Since the transformation of iron sand to hematite can be conducted by hydrothermal synthesis, It can improve the economic value of iron sand.

This study was aimed to evaluate the transformation of crystal structure of iron sand using hydrothermal synthesis. Moreover, evaluation the best raw material (iron sand or $Fe(OH)_x$ that extracted from iron sand) was carried out to attain the high purity of hematite. The heating temperature and time hydrothermal reaction were also evaluated to understand the oxide iron crystal transformation.

EXPERIMENTAL PROCEDURE

Iron sand taken by magnet of 10 mg was added with 100 mL of concetrated Hydrochloric acid (37%, merck). The mixture was heated at 70 °C in constant stirring for 1 h. Then, the mixture was filtered and the filtrate was added with 4 M of NaOH (Merck) in mole rasio 1 : 3. The obtained product was dark chocolate coloid $Fe(OH)_x$. Afterwards, the coloid was transfered to teflon lined stainless steel autoclave reactor, added with NaOH 2M of 30 mL, firmly sealed and heated. The hydrothermal reaction condition following Table 1. After the hydrothermal reaction, autoclaves were cooled at room temperature. Then, the samples were filtered and washed with deionized water. The solid product were dried at 60 °C for 12 h. Finally, the powder can be used for further analysis.

RESULT AND DISCUSSION

Effect of Hydrothermal Reaction Temperature

Iron sand from Paseban Beach, Jember, Indonesia has identified the crystal structure following X-Ray diffraction analysis. Figure 1.a - 1.d showed the diffractogram of the consecutive standard for α-Fe_2O_3, γ-Fe_2O_3, Fe_3O_4, and SiO_2 that was used as a comparison for the diffractogram of the sample product. Following the diffractogram of standard, iron sand has compounds such as SiO_2 (silica/quartz), α-Fe_2O_3, γ-Fe_2O_3, Fe_3O_4, and unidentified crystal structure (Figure 1.e). After separation using a magnet, the peaks of SiO_2 in Figure 1.f were absent (2θ = 26,65° and 39,52°), and remaining the iron oxides compounds (Fe_2O_3, and Fe_3O_4). All of the materials product obtained were analyzed the crystallinity by X-Ray diffaction technique (MPD X'pert PANalytical) using CuKα radiation 1.5405 Å. The samples were scanned in the diffraction angle 2θ = 10° - 60°.

[a] FHA. Hadi, T. Haryati, N. Andarini, S. Suwardiyanto, YA. Sulistiyo
Department of Chemistry, Faculty of Mathematics and Natural Sciences, University of Jember
*e-mail: yudi.fmipa@unej.ac.id

Table 1. reaction conditions and chemical used in the hydrothermal synthesis

Sample	Basic Resistance (Ohm)	Temperature (°C)	Time (h)
S1	1 g iron sand, 30 mL of NaOH 2M	160	24
S2	1 g iron sand, 30 mL of NaOH 2M	185	24
S3	1 g iron sand, 30 mL of NaOH 2M	210	24
S4	100 mL of coloid $Fe(OH)_x$, 30 mL of NaOH 2M	160	24
S5	100 mL of coloid $Fe(OH)_x$, 30 mL of NaOH 2M	185	24
S6	100 mL of coloid $Fe(OH)_x$, 30 mL of NaOH 2M	210	24
S7	100 mL of coloid $Fe(OH)_x$, 30 mL of NaOH 2M	160	36
S8	100 mL of coloid $Fe(OH)_x$, 30 mL of NaOH 2M	160	48

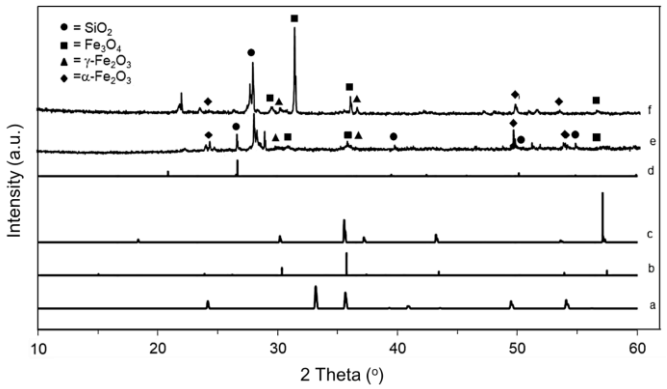

Figure 1. Diffractogram x-ray of, (a) α-Fe_2O_3 standard (R110013); (b) γ- Fe_2O_3 standard; (c) Fe_3O_4 standard (R061111); (d) SiO_2 standard (R100134); (e) iron sand; and (f) Magnetic separation of Iron sand

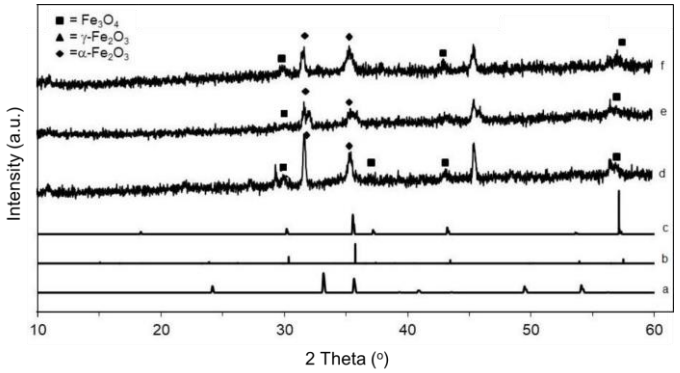

Figure 2. Diffractogram x-ray of (a) α- Fe_2O_3 standart (R110013), (b) γ- Fe_2O_3 standart, (c) Fe_3O_4 standart (R061111), sample at temperature reaction (d) 160 °C, (e) 185 °C, f). 210 °C, using raw material $Fe(OH)_x$ extracted from iron sand for 24 h time hydrothermal reaction

The transformation of the crystal phase that was identified by diffractogram x-ray was studied using different raw materials namely iron sand and $Fe(OH)_x$ from extracted iron sand in the thermal influence on the hydrothermal reaction. Figure 2 showed the polymorph crystal structures obtained using $Fe(OH)_x$ as a hydrothermal reaction source such as α-Fe_2O_3 and Fe_3O_4. The characteristic peaks of α-Fe_2O_3 can be identified at 2θ = 24.73, 33.18, 35.72, 38.23, 41.1, 49.63, and 54.24 which were similar to the database from rruff.info/hematite. Increasing of hydrothermal temperature (160 to 180 °C) reduced the peak intensity of α-Fe_2O_3 due to increasing the nucleation rate and decreasing the crystal size obtained. Increasing the temperature to 210 °C, the crystal of α-Fe_2O_3 was transformed to be a more stable structure namely Fe_3O_4 which can be seen by arising peaks at 2θ = 18.21, 30.20, 35.81, 36.76, 42.94, and 56.87 following rruff.info/magnetite. Zhang et al. (2013) also reported that γ-Fe_2O_3 was a more stable phase than α-Fe_2O_3 possibly form at the higher reaction temperature [16].

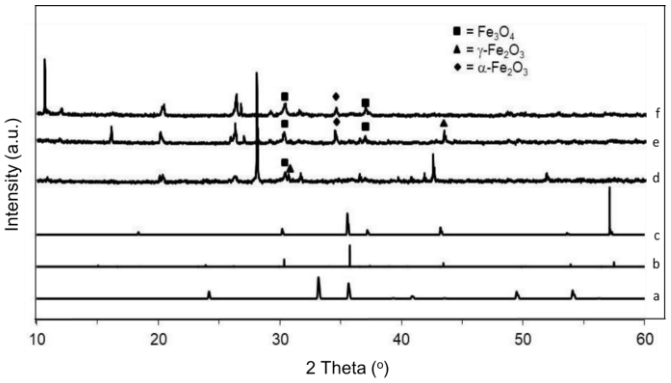

Figure 3. Diffractogram x-ray of (a) α-Fe_2O_3 standart (R110013), (b) γ-Fe_2O_3 standart, (c) Fe_3O_4 standart (R061111), sample at temperature reaction (d) 160 °C, (e) 185 °C, f). 210 °C, using raw material iron sand for 24 h time hydrothermal reaction

On the other hand, Figure 3 showed that the utilization of iron sand as raw materials for hydrothermal reaction produced more crystal structure compared to $Fe(OH)_x$ such as α-Fe_2O_3, γ-Fe_2O_3, Fe_3O_4, and silica (SiO_2). An additional crystal structure of γ-Fe_2O_3 was formed by increasing the reaction temperature. Meanwhile, a strong peak at 2θ = 27.90 can be addressed to silica that can be produced from the decomposition of Fe_2SiO_4 (Fayalite) by NaOH during the hydrothermal. During the hydrothermal, sodium silicate from the reaction of fayalite and NaOH was hydrolyzed and condensed producing a small amount of amorphous SiO_2. Sun et al (2018) reported that Fayalite is a product of the burning process in the magma chamber that is released in the eruption process [17]. Increasing the reaction temperature decreased the peak intensity of SiO_2 due to increasing the solubility of fayalite on NaOH that can be discharged in the filtration process.

Effect of Time Hydrothermal Reaction

The transformation of crystal structures was also evaluated by the various hydrothermal time reaction. The raw material usage was $Fe(OH)_x$ from the extracted iron sand which has the better result to produce α-Fe_2O_3 in the previous study compared to iron sand. Figure 4.c showed that high purity of α-Fe_2O_3 was obtained in 24 h of hydrothermal time reaction. It was indicated

from the characteristic peaks of α-Fe_2O_3 at 2θ = 31.75, 35.53, 45.52, dan 56.60. Increasing time reaction to 36 h was maintained of the α-Fe_2O_3 structure with the lower intensity of those peaks. Moreover, arising characteristic peaks of the crystal of γ-Fe_2O_3 and Fe_3O_4 that were followed by the absence of peaks α-Fe_2O_3 were observed in 48 h of time reaction. It was caused that the γ-Fe_2O_3 and Fe_3O_4 were the more stable phase than α-Fe_2O_3 [16].

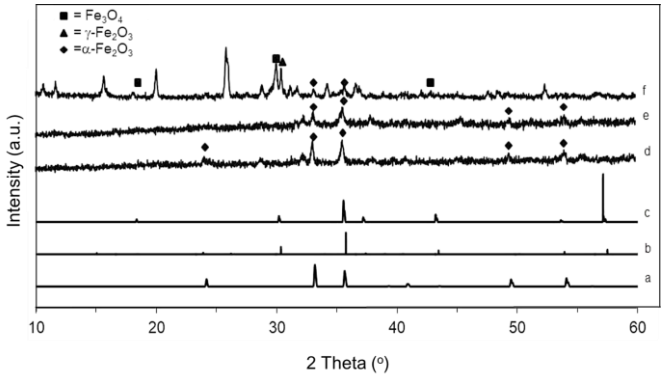

Figure 4. Diffractogram x-ray of (a) α-Fe_2O_3 standart (R110013), (b) γ-Fe_2O_3 standart, (c) Fe_3O_4 standart (R061111), sample at time reaction (d) 24 h, (e) 36 h, f). 48 h, using raw material $Fe(OH)_x$ extracted from iron sand at 160 °C of hydrothermal temperature

Decreasing α-Fe_2O_3 peaks and appearing γ-Fe_2O_3 and Fe_3O_4 phases was in line with Mikio et al., (2013) that reported the increasing hydrothermal time obtained the optimum condition at 32 h, meanwhile. the longer time reaction appearing the oxidation reaction to transform α-Fe_2O_3 to be γ-Fe_2O_3 phase [18]. Juliansyah et al. (2015) also reported that increasing time reaction increased the energy that accelerated the nucleation and crystal growth during the reaction to form a smaller crystal size. It also had a high possibility to transform the obtained crystal to be the more stable phase at the end of the rection process [19].

CONCLUSION

The ideal condition to attain the α-Fe_2O_3 phase by the hydrothermal reaction was using $Fe(OH)_x$ which was a product of the extraction of iron sand. The utilization of iron sand itself was triggered in producing multiphase in the reaction product. Increasing the temperature and time of hydrothermal reaction accelerates the transformation of α- Fe_2O_3 to γ- Fe_2O_3 and Fe_3O_4 phase. The best condition to attain high purity of α- Fe_2O_3 was at temperature reaction 160 °C for 24 h of time reaction.

REFERENCES

[1] S. Bijaksana, Z. Masrurah and S.J. Fajar, "Magnetic susceptibility and grain size distribution as prospective tools for selective exploration and provenance study of iron sand deposits: A case study from Aceh, Indonesia," *Heliyon*, vol 7, no. e08584, pp. 1-8, 2021.

[2] Kementerian ESDM Republik Indonesia, Peluang Investasi Besi Indonesia, Kemeterian Energi dan Sumber daya Mineral Republik Indonesia: Jakarta. 2022.

[3] Z. Zulhan, I.B.G.S. Adhiwiguna, A. Fuadi and N. Saleh, "Solid-state reduction of an Indonesian iron sand concentrate using subbituminous coal," *Canadian Metallurgical Quarterly*, vol. 60, no. 1, pp. 12-20, April 2021.

[4] R.L. Brathwaite, M.F. Gazley, A.B. Christie, "Provenance of titanomagnetite in ironsands on the west coast of the North Island, New Zealand," *Journal of Geochemical Exploration*, vol. 178, pp. 23-34, July 2017.

[5] A. Rozendaal, C. Philander and R. Heyn, "The coastal heavy mineral sand deposits of Africa," *South African Journal of Geology*, vol. 20, pp. 133-152, 2017.

[6] Kim, 2020 S. Kim, R. Bradshaw, P. Kulkarni, S. Allard, P.C. Chiu, A.R. Sapkota, M.J. Newell, E.T. Handy, C.L. East, K.E. Kniel and M. Sharma, "Zero-valent iron-sand filtration reduces escherichia coli in surface water and leafy green growing environments," *Frontiers in Sustainable Food Systems*, vol. 4, no. 112, pp. 1-11, July 2020.

[7] J. Chopyk, P. Kulkarni, D.J. Nasko, R. Bradshaw, K.E. Kniel, P. Chiu, M. Sharma and A.R. Sapkota, "Zero-valent iron sand filtration reduces concentrations of virus-like particles and modifies virome community composition in reclaimed water used for agricultural irrigation," *BMC Res Notes*, vol. 12, no. 223, pp. 1-8, 2019.

[8] P. Kulkarni, G.A. Raspanti, A.Q. Bui, R.N. Bradshaw, K.E. Kniel, P.C. Chiu, M. Sharma, A. Sapkota and A.R. Sapkot, "Zerovalent iron-sand filtration can reduce the concentration of multiple antimicrobials in conventionally treated reclaimed water," *Environmental Research*, vol. 172, pp. 301-309, 2019.

[9] H. Karami, "Synthesis and characterization of iron oxide nanoparticles by solid state chemical reaction method," *Journal of Cluster Science*, vol. 21, pp.11-20, 2010.

[10] S. Alagiri and S.B.A. Hamid, "Sol–gel synthesis of α-Fe_2O_3 nanoparticles and its photocatalytic application," *Journal of Sol-Gel Science and Technology*, vol. 74, pp. 783-789, 2015.

[11] M. Tadic, D. Trpkov, L. Kopanja, S. Vojnovic and M. Panjan, "Hydrothermal synthesis of hematite (α-Fe_2O_3) nanoparticle forms: Synthesis conditions, structure, particle shape analysis, cytotoxicity and magnetic properties," *Journal of Alloys and Compounds*, vol. 792, pp. 599-609, July 2019.

[12] F. Wang, X.F. Qin, Y.F. Meng, Z.L. Guo, L.X. Yang and Y.F. Ming, "Hydrothermal synthesis and characterization of α-Fe_2O_3 nanoparticles," *Materials Science in Semiconductor Processing*, vol. 16, no. 3, pp. 802-806, June 2013.

[13] Pan et al., 2009 Q. Pan, K. Huang, S. Ni, F. Yang, S. Lin and D. He, "Synthesis of α-Fe_2O_3 dendrites by a hydrothermal approach and their application in lithium-ion batteries," *Journal of Physics*, vol. 42, no. 1, pp. 1-5, 2009.

[14] W. Qin, C. Yang, R. Yi and G. Gao, "Hydrothermal synthesis and characterization of single-crystalline α-Fe_2O_3 nanocubes," *Journal of Nanomaterials*, vol. 2011, no. 159259, pp. 1-6, 2011.

[15] J. Chen, L. Xu, W. Li and X. Gou. "α-Fe_2O_3 nanotubes in gas sensor and lithium-ion battery applications," *Journal Advanced Materials*, vol. 17, no. 5, pp. 582-586, 2005.

[16] X. Zhang, Y. Niu, X. Meng, Y. Li and J. Zhao, "Structural evolution and characteristics of the phase transformations between α-Fe_2O_3, Fe_3O_4 and γ-Fe_2O_3 nanoparticles under reducing and oxidizing atmosphere," *Journal of CryEngComm*, vol. 15, pp. 8166-8172, 2013.

[17] Y. Sun, Z. Huiqun, Y. Kun, Z. Mengqi, X. Shijin, and L. Xiancai, "Transport properties of Fe_2SiO_4 melt at high pressure from classical molecular dynamics: implication for the lifetime of the magma ocean," *Journal of Geophysical Reaserch*, vol. 123, no. 5, pp. 1-40, 2018.

[18] K. Mikio, A. Kei, H. Akari, Y. Hideto, N. Yukio, and K. Eiji, "Characterization of spinel-structured iron oxide particles synthesized by heating γ-Fe_2O_3 platelets in tetra-ethylene glycol," *Material Transaction*, vol. 54, no. 2, pp. 222-224, 2013.

[19] Juliansyah, Ratnawulan, and F. Ahmad, "Pengaruh temperatur kalsinasi terhadap struktur mineral granit yang terdapat di Nagari Surian Kecamatan Pantai Cermin Kabupaten Solok," *Pillar of Physics*, vol 6, pp. 9-16, 2015.